Lightning Strikes and Prehistoric Ovens: Determining the Source of Magnetic Anomalies Using Techniques of Environmental Magnetism

David Maki*

Archaeo-Physics, LLC, 1313 5th Street SE, Minneapolis, Minnesota 55414

Techniques of environmental magnetism were used to examine soil samples from a North American archaeological site in an effort to determine the source of magnetic field gradient anomalies. Testing revealed the source of one anomaly to be lightning-induced remanent magnetization (LIRM). This anomaly had initially been identified as a possible archaeological feature, but excavations were unable to identify a visible source. LIRM appears to be a relatively common source of anomalous signal on archaeological sites, and may often be misinterpreted in magnetic imagery. Thermoremanent magnetization (TRM) was also documented and quantified in soil from archaeological hearths at the site, as were changes in the ferrimagnetic mineral concentration and coercivity spectra resulting from high-temperature enhancement within the hearths.

INTRODUCTION

A magnetic field gradient survey was conducted at 30-30 Winchester (48CA3030), a prehistoric archaeological site located in the Powder River Basin of northeastern Wyoming. The objective of the survey was to locate and map buried archaeological features associated with the prehistoric occupation of the site.

The site was occupied during the Late Prehistoric I by people who used a distinctive style of cylindrical pit hearth/oven, and also made what are assumed to be figurines made of baked clay, although these objects were too fragmented to determine their original shapes (Munson, 2002).

A magnetic survey (vertical gradient) was completed over approximately 3900 m^2 of the site using a Geoscan Research FM36 fluxgate gradiometer. Data were collected at 8 samples per meter along transects separated by 0.5 m. Results from a portion of this survey are presented in Figure 1. The geophysical survey successfully mapped 10 magnetic anomalies that were subsequently excavated during the archaeological mitigation of the site. Excavation revealed the source of the magnetic anomalies to be small-diameter cylindrical pit hearths/ovens with calibrated radiocarbon dates ranging from A.D. 300 to A.D. 1000 (Munson, 2002).

*E-mail: mark@archaeophysics.com.

Geoarchaeology: An International Journal, Vol. 20, No. 5, 449–459 (2005)

Published online in Wiley Interscience (www.interscience.wiley.com). DOI:10.1002/gea.20059

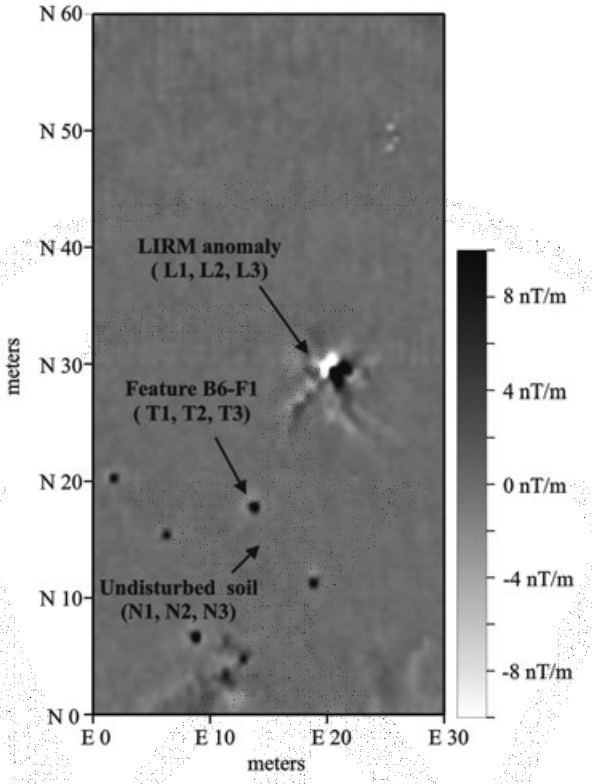

Figure 1. A magnetic field gradient image showing the suspected LIRM anomaly and several archaeological hearths. Consolidated soil samples were collected for laboratory analysis from Feature B6-F1 (dating to A.D. 680 ± 50), the LIRM anomaly, and undisturbed soil.

The pit hearths/ovens created circular magnetic anomalies approximately 1.5 m in diameter (Figure 1). The intensity of these anomalies ranged from –2 to +19 nanoteslas per meter (nT/m).

One atypical magnetic anomaly was also identified in the geophysical survey results (Figure 1). This anomaly was larger and more complex than anomalies associated with the archaeological hearths, and was composed of higher-intensity bipolar signal (±30 nT/m). An excavation unit was centered over this anomaly and excavated to a depth of 100 cm below surface (cmbs), without encountering a visible source. Examination of the soil profile revealed no variation from the undisturbed soil profiles at the site.

Because excavations at the location of the atypical anomaly in Figure 1 failed to detect visible evidence of archaeological features or artifacts, a geologic contrast, a modern disturbance, or a natural disturbance that might explain the observed anomaly, lightning-induced remanent magnetization (LIRM) was suspected as a possible

source. LIRM has been documented in soil, rock, brick, and concrete in the vicinity of lightning strikes (Cox, 1961; Graham, 1961; Dunlop et al., 1984; Sakai et al., 1998; Verrier and Rochette, 2002). LIRM is an isothermal remanent magnetization that occurs within a few meters of a lightning strike. The magnetic field created by the lightning discharge current can impart a secondary magnetization, overprinting the natural remanent magnetization (NRM) of the materials in the immediate vicinity. A lightning overprint is usually recognizable by its extreme intensity compared to the NRM that it replaces.

Bevan (1995) predicts that LIRM may be recognized by spatial characteristics of the resulting anomaly. For vertical currents, the magnetic anomaly will be bipolar, with equal amplitudes for the high and low components, while horizontal currents will produce a long bipolar anomaly along the length of that current.

This paper evaluates the suspected LIRM by the criteria developed by Dunlop et al. (1984), Wasilewski and Kletetschka (1999), and Verrier and Rochette (2002). Remanent and in-field magnetic properties of soil from archaeological hearths and the suspected LIRM site are compared, as are their coercivity spectra. High temperature mineralogical transformations within the archaeological hearths are quantified, and the relative frequency with which LIRM anomalies are detected during geophysical investigations of archaeological sites is discussed.

ROCK MAGNETIC METHODS FOR IDENTIFYING LIRM

An analysis of soil samples collected during the excavation of 30-30 Winchester was conducted in an effort to identify the source of magnetic anomalies at the site. The analysis consisted of two parts:

1. An examination of the characteristics of the NRM found in consolidated soil samples recovered during the excavation of 30-30 Winchester. Consolidated soil samples are defined, for the purposes of this article, as samples that have been excavated and conserved as a cohesive mass. The orientations of these samples were not recorded as they were collected. This was not a factor, however, as the analysis did not measure inclination or declination of the remanence found in the consolidated soil, but rather focused on the intensity of magnetization and characteristics of the magnetic minerals carrying the magnetic remanence.
2. An examination of the bulk magnetic properties of unconsolidated soil samples obtained from Winchester 30-30. These loose, non-cemented soil samples were recovered and bagged during excavation of the site. This analysis focused on the magnetic mineral concentration, grain size, and mineralogy of these samples in an effort to determine whether a susceptibility contrast associated with thermally induced mineralogical enhancement had occurred in the vicinity of the observed magnetic anomalies.

The analysis of consolidated soil samples utilized criteria for identifying LIRM previously developed by Dunlop et al. (1984), Wasilewski and Kletetschka (1999), and Verrier and Rochette (2002).

The criteria for the identification of LIRM suggested by Dunlop et al. (1984) and Wasilewski and Kletetschka (1999) include the following:

- REM values larger than 0.2. REM is defined as the ratio of NRM to that of a laboratory-imparted isothermal remanence using an applied field of 1 T (IRMs). Such intensities are much too large to have originated as TRM or chemical remanent magnetization (CRM). All other REMs are much less intense, tending to fall between 0.01 and 0.05.
- Koenigsberger ratios that lie between 10 and 100. Non-LIRM samples should possess a Koenigsberger ratio < 10. The Koenigsberger ratio Q_n is the ratio of remanent magnetization to the magnetization induced in the presence of the geomagnetic field of the Earth (H). A large Q_n value suggests isothermal remanence may be the primary source of the observed magnetic signal, while a low Q_n value suggests the anomalous signal may be related to induced magnetization caused by a susceptibility contrast. The parameter is defined as follows:

$$Q_n = \text{NRM}/[(\text{mass magnetic susceptibility}, \chi) \times H] \quad (1)$$

- Magnetization of the high-coercivity component of samples. One measure of this is the shape of the alternating field (AF) demagnetization curve of a sample. Relatively hard decay curves with SD-type curvatures (for example, an initial plateau before beginning to decay rapidly) suggest that relatively hard SD minerals and/or high coercivity minerals, such as hematite or goethite, are carrying at least some of the magnetic remanence. Soft, MD-type exponential decay curvatures suggest the magnetic remanence not carried by all the magnetic minerals in an assemblage, but only by the soft, MD ones.

More recently, Verrier and Rochette (2002), Gattacceca et al. (2003), and Gattacceca and Rochette (in press) have argued that the REM value is not well adapted to evaluate multicomponent magnetizations with different coercivity spectra. They argue that it is much more relevant to discuss the derivative REM value (which they term REM'). In the REM' method, the derivative of the AF demagnetization curve (dNRM/dAF) is normalized by the derivative of the AF demagnetization curve of a sample that has been given a laboratory imparted IRM ($dIRM_s/dAF$). Plots depicting the REM' value versus AF field should show decreasing values, followed by a slope breakdown at the point where the direction of magnetization changes from LIRM to NRM. The point at which this change in slope occurs identifies the LIRM destructive field, which can then be used to estimate the lightning discharge current. LIRM samples should possess maximum REM' values greater than 0.1, while other forms of natural magnetic remanence should possess maximum REM' values less than 0.1.

Soil Sample Descriptions

Unconsolidated samples were collected from six of the archaeological hearths, the suspected LIRM site, and several undisturbed locations. The unconsolidated soil was used to compare magnetic properties relating to magnetic mineral con-

centration, grain size, and composition. In addition, consolidated samples were collected from one archaeological hearth, the suspected LIRM site, and an undisturbed area; these samples were used to examine magnetic remanence properties and characteristics.

Several consolidated samples of oxidized soil were collected from within Feature B6-F1 (samples T1, T2, and T3). This feature was typical of the hearth/ovens, and is described as follows (Munson, 2002: 6-9–6-13):

> Feature B6-F1 is a small diameter pit hearth/oven. The top of the feature is 10 cmbs. The pit is circular in planview, has a straight wall, a flat bottom, and has the shape of a cylinder. The pit measures 48 cm in diameter and is 32 cm deep. Digging tool marks can be seen in a pit wall. Perhaps a digging stick or elk antler tine was used to dig the pit. As is typical of this type of feature, the pit is lined with two concentric bands of different color oxidized soil. The outer band is less than 1 cm to 3 cm thick, and is red (2.5YR4/6) in color, the inner band is less than 1 cm thick to 2 cm thick and is light red (2.5YR6/8) in color. The oxidized soil does not extend to the bottom of the pit.
>
> Eight sandstone slabs found in the pit weigh 6 kg. The largest rock measures 20 cm across and weighs 1.9 kg. Two of the rocks were lying near the top of the pit and the rest were lying on the bed of charcoal on the bottom of the pit. Except on the southern edge of the pit, the rocks are placed tightly together forming a barrier between the charcoal bed and the soil above the rocks. It is likely that the rocks were placed on top of the coals in preparation for the feature to be used as an oven.

Consolidated soils were collected from 30–55 cmbs at the suspected LIRM site (samples L1, L2, and L3). The soil profile from this excavation unit is described as follows (Munson, 2002: 2-6–2-7):

> The Ab soil horizon is from 0–30 cmbs. The soil is light brownish gray sand (10YR6/2) that is very well sorted. The soil includes silt and minor amounts of medium-sized sand grains. The Bk soil horizon is from 30 to 97 cmbs and consists of 1 to 2 cm thick horizontal layers composed of massive to finely laminated sand. The upper soil in the Bk soil horizon is a light brownish gray (10YR6/2) and the lower soil is a pale brown (10YR6/3).

Consolidated soil samples were collected from approximately 25 cmbs at an undisturbed soil location (samples N1, N2, and N3). The soil profile was similar to that described for the LIRM sample location.

MAGNETIC TESTING RESULTS

Remanence Properties

The remanent magnetizations of consolidated soil samples are presented in Table I, as are the REM and Koenigsberger ratios of these samples. Table I clearly shows samples from the suspected LIRM site possess a remanent magnetization much larger than the remaining samples. These samples also possess REM and Koenigsberger ratios that satisfy the criteria presented by Dunlop et al. (1984) and Wasilewski and Kletetschka (1999), except for the REM value of sample L1 which is slightly less than 0.2.

Table I. Remanent magnetization properties of selected consolidated samples.

Sample	Magnetization $\times 10^{-5}$ (Am^2/kg)	REM	Koenigsberger
LIRM (L1)	11.00	0.150	25.8
LIRM (L2)	16.00	0.230	38.8
LIRM (L3)	16.00	0.220	36.2
TRM (T1)	1.70	0.009	1.6
TRM (T2)	1.90	0.010	1.8
TRM (T3)	1.80	0.009	1.7
NRM (N1)	0.39	0.006	1.3
NRM (N2)	0.29	0.004	1.0
NRM (N3)	0.22	0.003	0.8

In Figure 2, the AF demagnetization curves of one suspected LIRM sample (L2) and one suspected TRM sample (T3) are compared. The LIRM sample has a relatively hard curve shape, with an initial plateau followed by a rapid decline. The shape of the curve indicates the high-coercivity component of this sample was magnetized, as might be expected to occur during a lightning strike. The AF demagnetization curve of the TRM sample displays a relatively "soft" exponential decline. The shape of this curve suggests low-coercivity minerals are the primary carriers of magnetic remanence in this sample.

REM' was also determined for one suspected LIRM sample (L2) and one suspected TRM sample (T3). The maximum REM' value of sample L2 was determined to be 1.5, well above the 0.1 threshold for LIRM suggested by Verrier and Rochette (2002). By comparison, the maximum REM' value for sample T3 was 0.06. A plot of REM' values versus AF fields for sample L2 revealed decreasing values; however, the plot lacked a slope breakdown. The lack of a change in slope suggests the sample was saturated by a very large magnetic field associated with the lightning strike, or possibly was struck many times. It is difficult to say for certain that the sample was truly saturated, as the common magnetic mineral goethite (and some goethite/hematite mixtures) can continue to acquire remanence at applied fields well in excess of 4 Tesla (France and Oldfield, 2000). It is, however, certain that the lack of a change in slope prevented us from estimating the LIRM destructive field, making an estimate of the lightning discharge current unfeasible.

Bulk Magnetic Properties

The magnetic mineral concentration, relative grain size, and composition of samples from several locations were compared in an effort to understand whether factors other than isothermal remanence might have contributed to the atypical magnetic anomaly. Figure 3 is a bivariate plot of mass magnetic susceptibility (χ) versus the anhysteretic susceptibility (χ_{ARM}). Such plots, often informally referred to as King plots, are a useful means of showing relative variation in magnetic mineral concentration and grain size (King et al., 1982). The relatively large χ and χ_{ARM} val-

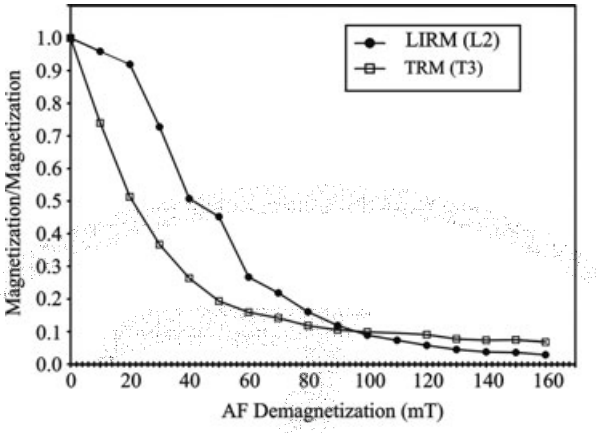

Figure 2. Alternating field (AF) demagnetization curves from the LIRM and TRM samples. The suspected LIRM sample exhibits a relatively hard SD-type curvature, while the TRM sample decreases exponentially.

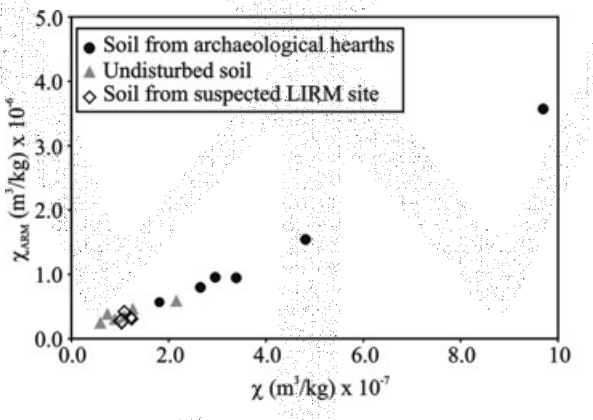

Figure 3. Bivariate plot of χ_{ARM} vs. χ. The similar values from undisturbed samples and samples from the suspected LIRM anomaly suggests little to no variation in the relative concentration and grain size of ferrimagnetic minerals, while soil from the archaeological hearths has experienced significant enhancement of the ferrimagnetic mineral component.

ues observed in oxidized soil from the archaeological hearths indicate an increased concentration of ferrimagnetic minerals, while the remaining samples show very little variation in ferrimagnetic mineral concentration. The increased concentration of ferrimagnetic minerals found in the hearth samples is most likely the result of high-temperature mineralogical enhancement of soil associated with these features. Dalan and Banerjee (1998) and Weston (2002) provide summaries of enhancement pathways of soils in an archaeological context. The data in Figure 3 fall on a single

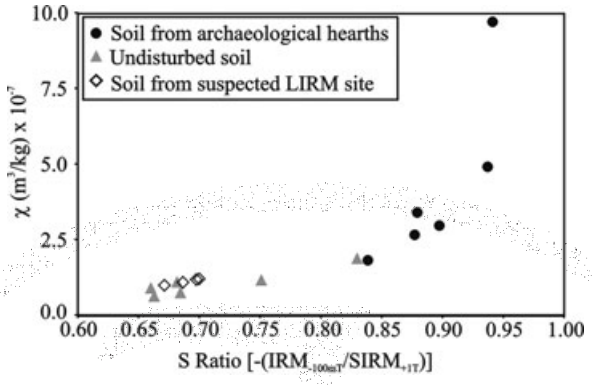

Figure 4. Bivariate plot of χ vs. S-Ratio. The mineralogy of undisturbed and LIRM samples is quite similar. The relative proportion of ferrimagnetic to canted antiferromagnetic minerals is much higher in soil from the archaeological hearth.

line, indicating the ferrimagnetic minerals produced during the enhancement process are of a very similar grain size to the ferrimagnetic minerals present prior to enhancement, probably around 0.2 μm.

Figure 4 is a bivariate plot of χ versus the S-Ratio. The S-Ratio is a backfield parameter defined here as: $-[IRM_{-100\ mT}/IRM_{+1T}]$<zaq;2>. It is an effective means of measuring relative variation in magnetic mineralogy (Harvey et al., 1981). Larger positive values imply a higher proportion of ferrimagnetic minerals, while smaller positive values (and occasional negative values) indicate an increasing concentration of canted antiferromagnetic minerals. Examination of Figure 4 reveals that samples from the archaeological hearths have a relatively greater proportion of ferrimagnetic minerals than the remaining samples. Again, this appears to indicate that significant high temperature mineralogical enhancement has occurred in oxidized soil associated with the prehistoric hearths.

A method of unmixing magnetic mineral assemblages was used to further examine the mineralogy of the samples and quantify their coercivity spectra. An analysis of spline smoothed isothermal remanent magnetization acquisition curves was completed using an automated unmixing procedure based on the expectation-maximization algorithm (Heslop et al., 2003). A two-component model was assumed. Results of the unmixing study are presented in Figure 5 and in Table II.

The unmixing study clearly reveals discrete low- and high-coercivity components in the natural magnetic mineral assemblage, with the high-coercivity component (Component 2) contributing approximately 40% of the magnetic mineral assemblage. The unmixing results from the hearth samples no longer show a significant high-coercivity component. This difference in coercivity spectra between the two soils dramatically quantifies the high-temperature ferrimagnetic mineral enhancement has taken place in soils associated with the archaeological hearths.

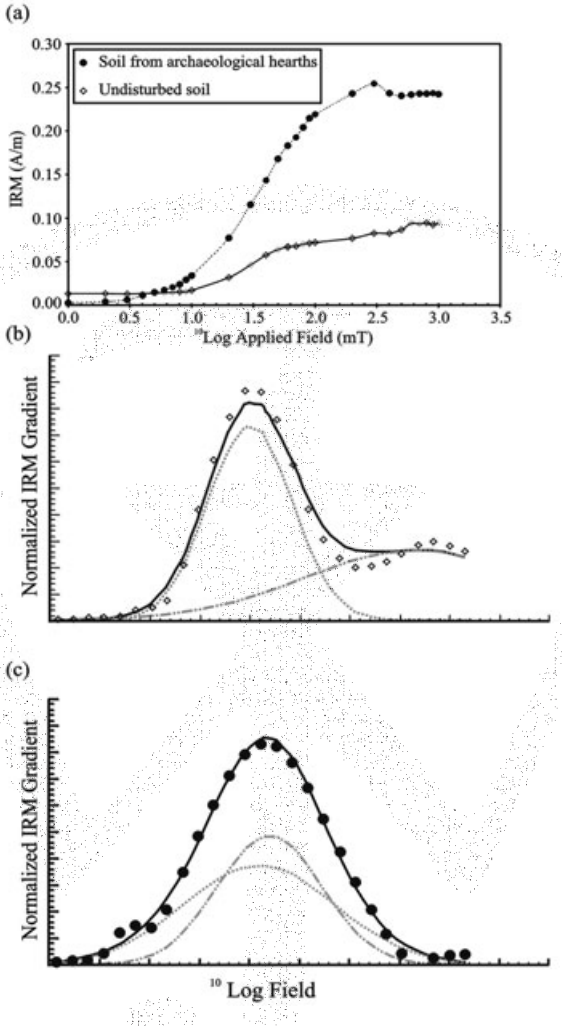

Figure 5. Results of the unmixing study: (a) IRM acquisition curves, (b) normalized IRM gradient from undisturbed soil, (c) normalized IRM gradient from hearth samples. Best fit model components are indicated by dashed lines.

Table II. Results of the unmixing study.

Sample	Component	log ($B_{1/2}$)	$B_{1/2}$ (mT)	DP	Contribution (%)
Natural soil	1	1.42	26	0.3	60
Natural soil	2	2.60	398	0.8	40
Hearth soil	1	1.48	30	0.5	53
Hearth soil	2	1.56	36	0.4	47

CONCLUSIONS

Laboratory testing of soil samples obtained from near the center of the atypical anomaly in Figure 1 has determined the source of the observed magnetic anomaly was lightning-induced isothermal remanent magnetization (LIRM). A review of magnetic survey data collected by the author over the past several years has identified several suspected LIRM anomalies. Although the laboratory magnetism data presented in this article represent the only formal attempt by the author to identify a LIRM anomaly, it is suspected that LIRM may be a relatively common source of magnetic signal on archaeological sites. Signal characteristics of LIRM that may help archaeological geophysicists identify these anomalies in the field are discussed in an upcoming publication (Jones and Maki, in press), as are several additional images of LIRM anomalies from archaeological sites.

LIRM was identified as the source of the anomaly based on the criteria of Dunlop et al. (1984), Wasilewski and Kletetschka (1999), and Verrier and Rochette (2002). The data meeting these criteria are summarized as follows:

- The average REM value ($n = 3$) of the LIRM samples is 0.2.
- The average Koenigsberger ratio ($n = 3$) is 33.6.
- The AF demagnetization curve has a hard, SD-type curvature.
- The REM' value is 1.5.

Additional evidence supporting the LIRM interpretation was provided by analysis of unconsolidated soil samples. Testing revealed little to no variation in magnetic mineral concentration, grain size, or composition between the LIRM samples and undisturbed soil from the site, while excavation revealed no fusion or high-temperature discoloration of the soil. This suggests that induced magnetization due to a susceptibility contrast was not a factor, leaving isothermal magnetization imparted by an intense magnetic field as the probable source of the observed anomaly.

Analysis of samples collected from an archaeological hearth shows the soil retained a TRM for some 1300 years. The intensity of this TRM was approximately six times greater than the intensity of nearby NRM. High-temperature mineralogical transformations within the heated soil surrounding the hearths increased the concentration of ferrimagnetic minerals. Changes to the coercivity spectra of these minerals are summarized in Figure 5 and Table II.

The data presented in this paper should be of assistance to others in the interpretation of magnetic survey imagery from archaeological sites. The quantification of magnetic remanence and ferrimagnetic enhancement within the archaeological hearths may also be useful to those interested in modeling the magnetic signal from archaeological features.

I thank the personnel of the Institute for Rock Magnetism, University of Minnesota. The Institute for Rock Magnetism is supported by the USNSF and the W.M. Keck Foundation (Los Angeles). Thanks also to Bruce Bevan, Rinita Dalan, and Christoph Geiss for providing useful and informative comments on an early draft of this paper.

REFERENCES

Bevan, B. (1995). Magnetic surveys and lightning. Near-Surface Views (newsletter of the Near Surface Geophysics section of the Society of Exploration Geophysics, October 1995, 7–8.

Cox, A. (1961). Anomalous remanent magnetization of basalt. U.S. Geological. Survey Bulletin, 1083-E, 131–160.

Dalan, R., & Banerjee, S.K. (1998). Solving archaeological problems using techniques of soil magnetism. Geoarchaeology, 13, 3–36.

Dunlop, D J., Schutt, L.D., & Hale, C.J. (1984). Paleomagnetism of Archean rocks from northwestern Ontario: III. Rock magnetism of the Shelley Lake granite, Quetico Subprovince. Canadian Journal of Earth Science, 21, 879–886.

France, D.E., & Oldfield, F. (2000). Identifying geothite and hematite from rock magnetic measurments of soils and sediments. Journal of Geophysical Research, B2, 105, 2781–2795.

Gattacceca, J., Rochette, P., & Bourot-Denise, M. (2003). Magnetic properties of a freshly fallen LL ordinary chondrite: The Bensour meteorite. Physics of the Earth and Planetary Interiors, 140, 343–358.

Gattacceca, J., & Rochette, P. (in press). Toward a robust normalized magnetic paleointensity method applied to meteorites. Earth and Planetary Science Letters.

Graham, K.W.T. (1961), The re-magnetization of a surface outcrop by lightning currents. Geophysical Journal of the Royal Astronomical Society, 6, 85–102.

Harvey, A.M., Oldfield, F., & Baron, A.F. (1981). Dating of Post-Glacial landforms in the central Howgills. Earth Surface Processes and Landforms, 6, 401–412.

Heslop, D., Dekkers, M.J., Kruiver, P.P., & van Oorschot, I.H.M. (2002). Analysis of isothermal remanent magnetization acquisition curves using the expectation–maximization algorithm. Geophysical Journal International, 148, 58–64.

Jones<zaq;1> & Maki, D. (in press). Lightning induced magnetic anomalies on archaeological sites. Archaeological Prospection.

King, J., Banerjee, S.K., Marvin, J., & Ozdemir, O. (1982). A comparison of different magnetic methods of determining the relative grain size of magnetite in natural materials: Some results from lake sediments. Earth and Planetary Science Letters, 59, 404–419.

Munson, G. (2002). Excavation of 3030 Winchester. Bozeman, MT: GCM Services.

Sakai, H., Sunada, S., & Sakurano, H. (1998). Study of lightning current by remanent magnetization. Electrical Engineering in Japan, 123, 41–47.

Verrier, V., & Rochette, P. (2002). Estimating peak currents at ground lightning impacts using remanent magnetization. Geophysical Research Letters, 29, 14-1–14-4.

Wasilewski, P., & Kletetschka, G. (1999). Lodestone: Nature's only permanent magnet—What it is and how it gets charged. Geophysical Research Letters, 26, 2275–2278.

Weston, D.G. (2002). Soil and susceptibility: Aspects of thermally induced magnetism within the dynamic pedological system. Archaeological Prospection, 9, 207–215.

Received April 2, 2004
Accepted for publication June 18, 2004

QUERIES

<<enote>>AQ1: Please supply author initial(s).

<<enote>>AQ2: Equation in text doesn't match figure (–[$IRM_{-100\,mT}$/IRM_{+1T}] in text and [–$IRM_{-100\,mT}$/$SIRM_{+1T}$] in Figure) Which is correct?